A Fully Integrated Multiconductor Model for TLM

A. James Wlodarczyk, Vladica Trenkic, *Member, IEEE,* Richard A. Scaramuzza, and Christos Christopoulos, *Member, IEEE*

***Abstract*— A fully integrated model of coupling between the electromagnetic field and multiconductor cabling is developed using the transmission-line matrix (TLM) method. In this model, the multiconductor cables are represented by multiconductor transmission lines which connect to the general TLM mesh. A basic TLM model of straight multiconductor lines is developed first, followed by the derivation of a general multiconductor junction model suitable for describing more complex configurations. Sample numerical results are presented to confirm validity and efficiency of the model.**

***Index Terms*—Multiconductor transmission lines, time-domain analysis, transmission-line matrix methods.**

I. Introduction

VERY OFTEN, particularly in electromagnetic compatibility studies, there is a need to model multiconductor cables which couple with the electromagnetic field. The main difficulty, as far as time-domain transmission-line matrix (TLM) and finite-difference time-domain (FDTD) method are concerned, is that it can be prohibitively inefficient to model the fine detail of closely spaced conductors in a large volume of space such as the interior of an equipment cabinet or room. A common technique used to incorporate multiconductor cables into differential time-domain techniques is the so-called separated solution [1], in which the multiconductors are treated separately from the rest of the problem, allowing for field coupling to the wires by introducing equivalent sources derived from a knowledge of the incident field. Although this method is simple, it involves several restrictions, the most important being that any electromagnetic interaction of the wires with the rest of the structure must be negligibly small.

Recently, an integrated solution, allowing for two-way coupling between the field and single thin wires, has been introduced in the TLM [2], [3]. Here, the propagation of signals along the wire is modeled by using special wire networks constructed by additional TLM link and stub lines. Such wire networks are interfaced with the ordinary three-dimensional condensed TLM nodes during the usual time-stepping procedure.

In this paper, we extend the TLM integrated thin-wire model to allow for modeling of multiconductor cables. We choose to regard the multiconductor transmission lines used in the TLM model as *vector lines*, i.e., lines which carry a signal, which is an *n-dimensional vector*, rather than a scalar function of time. This terminology is concise and helps to distinguish the TLM multiconductor transmission lines from the multiconductor cables being modeled. We consider the possible network connections (shunt and series) between vector lines and between vector and scalar lines before presenting the integrated TLM multiconductor cable model. The development of a basic model of straight multiconductor lines is presented first, followed with the derivation of a general multiconductor junction model, which can be used to model more complex configurations found in practice. Validity, efficiency, and versatility of the new model are tested by modeling electromagnetic compatibility of equipment boxes and the magnetic field around a solenoid.

Manuscript received March 27, 1998; revised August 27, 1998.

A. J. Wlodarczyk, V. Trenkic, and R. A. Scaramuzza are with KCC Ltd., Nottingham NG16 3BF, U.K.

C. Christopoulos is with the School of Electrical and Electronic Engineering, University of Nottingham, Nottingham NG7 2RD, U.K.

Publisher Item Identifier S 0018-9480(98)09192-3.

II. Basic TLM Multiconductor Model

A general multiconductor line consists of a number of parallel conductors of arbitrary cross section, but uniform in the third dimension. The state of an $n+1$ conductor line (carrying TEM or quasi-TEM modes only, and neglecting the common mode), can be specified by n voltages and n currents at each point along its length. It is convenient to assume that the n voltages, chosen to specify the state of the line, are the voltages of n of the conductors, with respect to the $(n+1)$th (reference) conductor, while the currents are the currents on the same n conductors in the direction of propagation. These currents and voltages can be represented by two n component vectors, I and V, while the line can be characterized by per-unit-length capacitance and inductance matrices C and L [4].

Following the approach used in the TLM model of a thin single wire [2], we can assume that one part of the required per-unit-length capacitance and inductance of an n-conductor line is already modeled by the single column of TLM cells through which it passes. This can be accounted for in a TLM model by placing a fictitious cylinder sheath around the multiconductor line, which can be taken as the reference conductor, or $(n+1)$th conductor line. Its diameter is the effective diameter of a column of metal-filled TLM cells, which is, unfortunately, different for capacitance and inductance, with the "capacitance shell" radius r_C being greater than the "inductance shell" radius r_L [2]. Notice that common-mode currents are accounted for in this model—the body of the TLM mesh refers any distant return paths to the sheath, while including all the effects of intervening metal or dielectric structures and sources.

The basic parameters, therefore, needed for the TLM model are C_d, the $n \times n$ distributed-capacitance matrix for the n-conductor cable placed inside the r_C radius reference con-

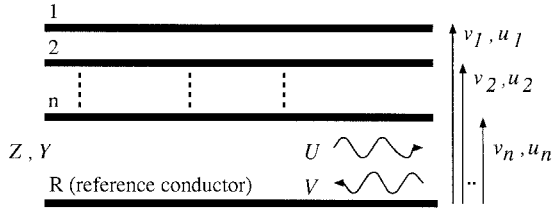

Fig. 1. A TLM vector line.

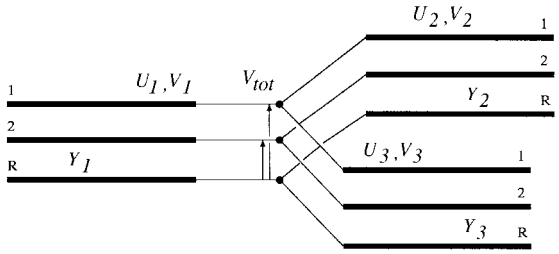

Fig. 2. Shunt connection of three two-conductor TLM vector lines.

ductor, and L_d, the $n \times n$ distributed-inductance matrix for the n-conductor cable placed inside the r_L radius reference conductor. Calculation of L_d and C_d requires solution of a two-dimensional electrostatic problem in the cross section of the multiconductor line. In the general case, this cannot be done analytically, but well-defined numerical techniques are available [4].

In order to facilitate integrated modeling of multiconductor structures in the TLM, we need to introduce new TLM elements carrying a signal which is n-dimensional vector. As explained in Section I, we regard these lines as TLM vector lines (as opposite to ordinary or scalar TLM lines) and they can be either *vector link lines* or *vector stub lines*. An n-element TLM vector line (link or stub) is depicted in Fig. 1 and is characterized by an $n \times n$ impedance matrix Z (or $n \times n$ admittance matrix $Y = Z^{-1}$), while its state is described by n-element incident and reflected voltage pulse vectors U and V, respectively. Possible network connections, shunt and series, between vector lines can be formulated directly from the first principles.

The shunt connection between n-element vector lines can be physically constructed by connecting n corresponding conductors in n junction points and having all vector lines sharing the same reference conductor. This is shown in Fig. 2 in the case of three two-element vector lines. In the general case of m n-element vector lines (labeled by $i = 1 \cdots m$), the total current into the junction must be the zero vector, i.e.,

$$I_{\text{tot}} = \sum_{i=1}^{m} Y_i (U_i - V_i) = 0 \tag{1}$$

while the total voltage at the junction is the sum of incident and reflected voltages

$$V_{\text{tot}} = U_i + V_i, \qquad \text{for all } i. \tag{2}$$

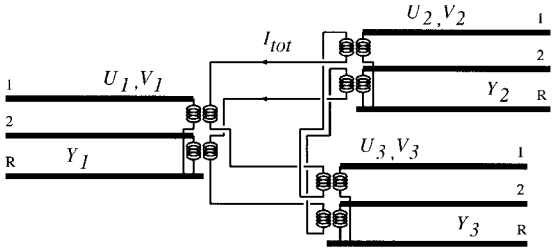

Fig. 3. Series connection of three two-conductor TLM vector lines.

Combining (1) and (2), we can describe a total voltage vector in terms of incident voltage vectors only as

$$V_{\text{tot}} = 2\left(\sum_{i=1}^{m} Y_i\right)^{-1} \sum_{i=1}^{m} Y_i U_i \tag{3}$$

and, hence, calculate reflected voltage pulses as

$$V_i = V_{\text{tot}} - U_i, \qquad \text{for all } i. \tag{4}$$

The series connection between vector lines can be constructed by using n 1:1 transformers at the end of each line (between the reference conductor and the other n conductors), to give n two conductor ports not sharing the same reference conductor, and then series connecting the corresponding ports of all the lines. This is shown in Fig. 3 in the case of three vector lines with two conductors. In the general case of m n-element vector lines, the total voltage around the junction is the zero vector, so

$$V_{\text{tot}} = \sum_{i=1}^{m} (U_i + V_i) = 0 \tag{5}$$

while the total current around the junction is

$$I_{\text{tot}} = Y_i (U_i - V_i), \qquad \text{for all } i. \tag{6}$$

Combining (5) and (6), we can express total current vector in terms of incident voltage vectors only as

$$I_{\text{tot}} = 2\left(\sum_{i=1}^{m} Z_i\right)^{-1} \sum_{i=1}^{m} U_i \tag{7}$$

and, hence, calculate reflected voltage pulses as

$$V_i = U_i - Z_i I_{\text{tot}}, \qquad \text{for all } i. \tag{8}$$

The principal TLM model of a segment of n-conductor cable is shown in Fig. 4. The cable and enclosing fictitious cylinder sheath form an $(n+1)$-conductor transmission line, which is modeled using a circuit of n-element vector lines. The cable is coupled to the external environment at the center of each TLM cell by a break in the sheath. The vector link lines of the impedance matrix Z_w can be chosen to model the total required capacitance of the wire segment of length Δx. To preserve the time synchronism of the TLM pulses imposed by the time step Δt, we must have $C_{\text{tot}} = C_d \Delta x = Z_w^{-1} \Delta t$, which gives

$$Z_w = \frac{\Delta t}{\Delta x} C_d^{-1}. \tag{9}$$

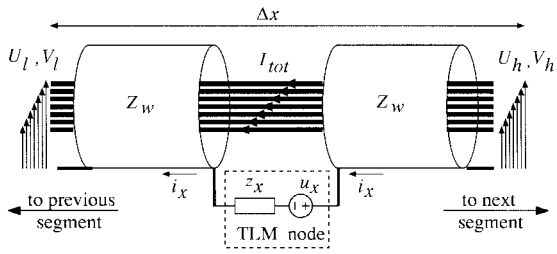

Fig. 4. TLM model of a multiconductor segment.

The inductance modeled by the vector link lines $Z_w\Delta t$ is normally insufficient [2], and a vector inductance stub of the impedance Z_s, connected in series to vector link lines, is required to make up the required total inductance given by

$$L_{\rm tot} = L_d\Delta x = Z_w\Delta t + Z_s\frac{\Delta t}{2}$$

from which it follows that

$$Z_s = 2\left(L_d\frac{\Delta x}{\Delta t} - Z_w\right). \tag{10}$$

The n-element vector inductance stub is not shown in the diagram due to the difficulty of drawing multiconductor series connections.

It can be seen from Fig. 4 that the coupling between the multiconductor cable model and the external environment is modeled using a voltage source in the reference line. The voltage source represents the electric-field component coupling with the multiconductor cable. Its amplitude u_x and the resistance z_x can be calculated from the incident voltage pulses and characteristics admittances of the relevant node's link and stub lines [5].

It is noted that the current in the reference conductor i_x is minus the sum of the currents in the other conductors, i.e., $i_x = -1_h I_{\rm tot}$, where 1_h is the single row matrix $(1, 1, \cdots, 1)$ and $I_{\rm tot}$ is the current through vector link lines. Similarly, the voltage drop v_{tx} on the reference conductor affects equally all the other lines, which can be described as $V_{tx} = 1_v v_{tx}$, where 1_v is the single-column matrix, the transpose of 1_h. Since $v_{tx} = u_x + z_x i_x$ and $i_x = -1_h I_{\rm tot}$, we write

$$V_{tx} = 1_v u_x - 1_v z_x 1_h I_{\rm tot} = U_x - Z_x I_{\rm tot}$$

which implies that a source in the reference line is equivalent to a vector source of $U_x = 1_v u_x$ and impedance matrix $Z_x = 1_v z_x 1_h$ connected in series with the other vector lines. (Note that U_x is a vector with all elements equal to u_x and Z_x is a singular matrix with all elements equal to z_x.)

Therefore, the model depicted on Fig. 4 can be realized as a series connection of four vector lines (two link lines, a stub, and a source). Using (7), we can express $I_{\rm tot}$ in terms of incident voltage pulses as

$$I_{\rm tot} = 2(2Z_w + Z_s + Z_x)^{-1}(U_h - U_l - U_s + U_x).$$

Using (8), voltage pulses reflected to the vector link lines (V_h and V_l) and the vector stub line (V_s) are calculated as

$$V_h = U_h - Z_w I_{\rm tot} \tag{11}$$

$$V_l = U_l + Z_w I_{\rm tot} \tag{12}$$

$$V_s = U_s + Z_s I_{\rm tot}. \tag{13}$$

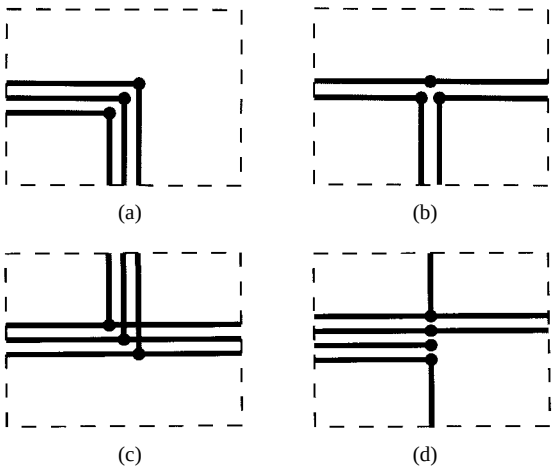

Fig. 5. Possible multiconductor configurations. (a) Multiconductor bend. (b) Branching-off. (c) Three T-junctions. (d) Combined T-junction, straight wire, termination, and bend.

Finally, the current flowing through the reference conductor $i_x = -1_h I_{\rm tot}$ is used to update voltage pulses on the ordinary node link and stub lines, following the method described in [5].

III. TLM Multiconductor Junction Model

In many situations, the model of straight multiconductor cables, described in Section II, may not be sufficient. Examples of when a more general model is required are shown in Fig. 5. They include multiconductor bends, branching-off configurations, multiconductor junction connections, discontinuation of some conductors or even arbitrary combinations of these features. As before, when modeling these configurations using the TLM, there will always be a common reference conductor—fictitious cylinder—which divides and follows every multiconductor branch. This makes it possible to devise a general multiconductor junction model based on the shunt connection of vector lines.

In a general multiconductor junction configuration there will be N junction points, where N is regarded as the order of the junction. In Fig. 5, we have $N = 3$ for (a)–(c) and $N = 4$ for (d). Every junction point may connect up to six single conductors coming from six different faces of a rectangular cell, referred to as "multiconductor limbs." A junction must be described by N-element vectors and matrices of size $N\times N$. However, quantities local to a particular limb, such as incident voltages and impedance matrices of the vector link lines, may already be described by vectors and matrices of order $n \le N$, where n represents the number of conductors actually present in that limb. The relative numbering of conductors local to a particular limb may, therefore, differ from that used for the junction as a whole. Thus, to obtain junction quantities of the order N, we need to reorder rows/columns of the local limb quantities and insert zeros in the rows/columns related to the nonexisting conductors. Such a transformation can be accomplished by using a limb permutation matrix P of size $N \times n$, which contains elements $P[i, j] = 1$ if the jth limb conductor connects to the ith junction point, and $P[i, j] = 0$ otherwise. A permutation matrix P must satisfy $P^T P = E$,

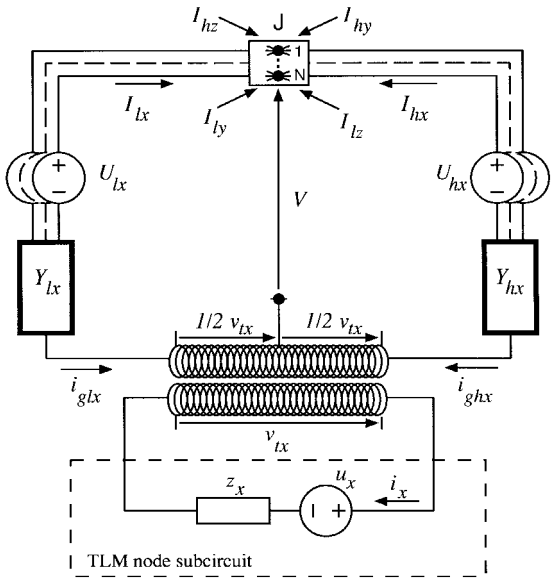

Fig. 6. Thevenin equivalent of multiconductor junction in the TLM (only a loop corresponding to limbs in the x-direction is shown).

where P^T is a transpose of P and E is a unitary matrix of size $n \times n$.

In general, the transformation of a vector A of size $n \times 1$ is performed by multiplying it with a permutation matrix P (size $N \times n$) to obtain an expanded vector PA of the size $N \times 1$. The original vector A is restored from the expanded one by multiplying it with P^T, i.e., $P^T(PA) = (P^TP)A = A$. A matrix M of size $n \times n$ can be transformed to a $N \times N$ matrix by applying PMP^T. The original matrix is restored from the expanded form by applying a reverse transformation, i.e., $P^T(PMP^T)P = (P^TP)M(P^TP) = M$.

The Thevenin equivalent of a general multiconductor junction model is shown in Fig. 6. For simplicity, only part of the circuit, corresponding to the limbs in the x-direction, is shown. This subcircuit is connected to the other two similar subcircuits, for y and z-directed limbs, via a multipoint junction, which is denoted by J. A transformer is introduced into each subcircuit to permit connection of the reference conductors at the center of the TLM node. The limbs are denoted by two letters, the first (c) indicating whether the limb is associated with the higher (h) or lower (l) value of the coordinate axis, and the second (k) indicating the coordinate axis, i.e., $k \in \{x, y, z\}$.

In the model from Fig. 6, every multiconductor limb is represented by the combination of vector link line and a vector stub line, connected in series, and is described by a single Thevenin equivalent circuit, (e.g., U_{lx}, Y_{lx}). The equivalent limb voltage vectors are then defined as

$$U_{ck} = P_{ck}(2U_{wck} + 2U_{sck}) \tag{14}$$

with indexes $c \in \{h, l\}$, $k \in \{x, y, z\}$, and where U_{wck} are incident voltage pulses from vector link lines, U_{sck} are incident voltage pulses from vector stub lines, and P_{ck} are permutation matrices discussed above. For completely absent limbs, U_{ck} is set to a null vector.

The corresponding limb admittance matrices Y_{ck} are defined as

$$Y_{ck} = P_{ck}(Z_{wck} + Z_{sck})^{-1}P_{ck}^T \tag{15}$$

where Z_{wck} are impedance matrices of vector link lines, which are calculated as in the straight segment model, using (9), while Z_{sck} are impedance matrices of vector stub lines, calculated as half of those used in the straight segment model, given by (10). For completely absent limbs, Y_{ck} is set to a null matrix. Note that the admittance matrix for each limb may become singular on expansion to the Nth order, due to the introduction of zero rows and columns associated with the absent conductors. However, it is easy to prove, taking into account the junction topology, that the sum of the admittance matrices for all the limbs associated with the junction is always a nonsingular matrix.

As before, the coupling with the external environment is modeled using equivalent voltage sources, which are calculated from the incident voltage pulses and characteristics admittances of the relevant node's link and stub lines [5]. A voltage source (u_k, z_k) couples with k-directed limbs of the multiconductor junction via an ideal transformer, as depicted in Fig. 6 for x-direction and the source (u_x, z_x). This voltage source causes a voltage drop of $v_{tx}/2$ in the reference conductor of a multiconductor limb. Voltage v_{tx} can be obtained from the node's side of the transformer as

$$v_{tx} = u_x + z_x i_x. \tag{16}$$

Since (from transformer rules)

$$i_x = \frac{1}{2}(i_{ghx} - i_{glx}) \tag{17}$$

and

$$i_{glx} = -1_h I_{lx} \qquad i_{ghx} = -1_h I_{hx} \tag{18}$$

we can write

$$v_{tx} = u_x + \frac{z_x}{2}\, 1_h(I_{lx} - I_{hx}). \tag{19}$$

The voltage drop $v_{tx}/2$ in the reference line affects all other lines of a multiconductor limb in the same way. This can be expressed by making use of (19) as

$$V_{gx} = \frac{1_v v_{tx}}{2} = \frac{U_x}{2} + \frac{1}{4}\, Z_x(I_{lx} - I_{hx}) \tag{20}$$

where $Z_x = 1_v z_x 1_h$ is a singular matrix with all elements equal to z_x and $U_x = 1_v u_x$.

Taking into account the voltage drop V_{gx}, we can now write voltage equations for the two loops of the x-directed limbs as

$$Y_{lx}(U_{lx} - V_{gx} - V) = I_{lx} \tag{21}$$

$$Y_{hx}(U_{hx} + V_{gx} - V) = I_{hx} \tag{22}$$

which, after substituting V_{gx} using (20) and generalizing for all directions ($x \to k$), can be written as

$$Y_{lk}\left(U_{lk} - \frac{U_k}{2} - V\right) = I_{lk} + \frac{1}{4}\, Y_{lk} Z_k(I_{lk} - I_{hk}) \tag{23}$$

$$Y_{hk}\left(U_{hk} + \frac{U_k}{2} - V\right) = I_{hk} + \frac{1}{4}\, Y_{hk} Z_k(I_{hk} - I_{lk}). \tag{24}$$

By introducing further substitutions,

$$W_{lk} = U_{lk} - U_k/2 \tag{25}$$
$$W_{hk} = U_{hk} + U_k/2 \tag{26}$$
$$J_{ck} = Y_{ck}(W_{ck} - V), \qquad c \in \{l, h\} \tag{27}$$

we can rewrite (23) and (24) as

$$J_{lk} = I_{lk} + \frac{1}{4}Y_{lk}Z_k(I_{lk} - I_{hk}) \tag{28}$$
$$J_{hk} = I_{hk} + \frac{1}{4}Y_{hk}Z_k(I_{hk} - I_{lk}). \tag{29}$$

Currents on the multiconductors limbs flowing into the junction are unknown N-element vectors, which must satisfy the current equation for the multipoint junction J

$$\sum_{k=x,\,y,\,z}(I_{lk} + I_{hk}) = 0. \tag{30}$$

Six loop equations derivable from (28) and (29) for $k \in \{x, y, z\}$ and the current equation for the junction J given by (30) represent a system of seven simultaneous matrix equations with seven unknown vectors: I_{lx}, I_{hx}, I_{ly}, I_{hy}, I_{lz}, I_{hz}, and V. It can be solved as follows.

After subtracting (29) from (28), we obtain

$$J_{lk} - J_{hk} = \left[E + \frac{1}{4}(Y_{lk} + Y_{hk})Z_k\right](I_{lk} - I_{hk}) \tag{31}$$

where E is an Nth order unitary matrix. This can be rewritten as

$$I_{lk} - I_{hk} = C_k(J_{lk} - J_{hk}) \tag{32}$$

where C_k is introduced as

$$C_k = \left[E + \frac{1}{4}(Y_{lk} + Y_{hk})Z_k\right]^{-1}. \tag{33}$$

Adding (29) to (28), we obtain

$$J_{lk} + J_{hk} = I_{lk} + I_{hk} + \frac{1}{4}(Y_{lk} - Y_{hk})Z_k(I_{lk} - I_{hk}). \tag{34}$$

By further substituting $(I_{lk} - I_{hk})$ from (32) and introducing

$$A_k = \frac{1}{4}(Y_{lk} - Y_{hk})Z_kC_k \tag{35}$$

we obtain

$$I_{lk} + I_{hk} = (E - A_k)J_{lk} + (E + A_k)J_{hk}. \tag{36}$$

We can now substitute (36) into (30) and obtain

$$\sum_{k=x,\,y,\,z}[(E - A_k)J_{lk} + (E + A_k)J_{hk}] = 0.$$

By recalling definitions (27), we rewrite the above equation as

$$\sum_{k=x,\,y,\,z}[(E - A_k)Y_{lk}W_{lk} + (E + A_k)Y_{hk}W_{hk}] = \left\{\sum_{k=x,\,y,\,z}[(E - A_k)Y_{lk} + (E + A_k)Y_{hk}]\right\}V.$$

Now introduce B matrices as

$$B_{lk} = (E - A_k)Y_{lk} \tag{37}$$
$$B_{hk} = (E + A_k)Y_{hk} \tag{38}$$

so we have

$$\sum_{k=x,\,y,\,z}(B_{lk}W_{lk} + B_{hk}W_{hk}) = \left[\sum_{k=x,\,y,\,z}(B_{lk} + B_{hk})\right]V. \tag{39}$$

Although the individual matrices B may be singular, it can be proven, as in the case of Y matrices, that $\sum_{k=x,\,y,\,z}(B_{lk} + B_{hk})$ is a nonsingular matrix. Thus, we can obtain V as

$$V = \left[\sum_{k=x,\,y,\,z}(B_{lk} + B_{hk})\right]^{-1} \cdot \left[\sum_{k=x,\,y,\,z}(B_{lk}W_{lk} + B_{hk}W_{hk})\right]. \tag{40}$$

Combining (32) and (36), the currents flowing into the limbs are easily obtained as

$$I_{lk} = \frac{1}{2}(E + C_k - A_k)J_{lk} + \frac{1}{2}(E - C_k + A_k)J_{hk} \tag{41}$$
$$I_{hk} = \frac{1}{2}(E + C_k + A_k)J_{hk} + \frac{1}{2}(E - C_k - A_k)J_{lk}. \tag{42}$$

In summary, once V is found using (40), we can calculate J_{lk} and J_{hk} using (27) and, subsequently, I_{lk} and I_{hk} by using the above two equations. By applying a reverse transformation matrix P_{ck}^T onto I_{ck}, we can discard zero elements related to the nonexisting conductors, thus producing the current vector $P_{ck}^TI_{ck}$ with elements consistent with a local labeling scheme for the particular limb of the junction.

After calculating limb current vectors, the voltage pulses reflected to vector stub and link lines are easily calculated (taking into account permutation matrices) as

$$V_{wck} = U_{wck} - Z_{wck}P_{ck}^TI_{ck} \tag{43}$$
$$V_{sck} = U_{sck} - Z_{sck}P_{ck}^TI_{ck}. \tag{44}$$

The current flowing through the TLM node's side of the transformer i_k where $k \in \{x, y, z\}$ can be found after generalizing and combining (17) and (18) as

$$i_k = \frac{1_h(I_{lk} - I_{hk})}{2} \tag{45}$$

which is used to update voltage pulses on the ordinary node's link and stub lines, following the method described in [5].

IV. Numerical Examples

In order to test the multiconductor model, we have modeled a structure with two equipment boxes and connecting wires, as depicted in Fig. 7. The wires and metal structure form a coupling mechanism between the four terminations or ports. By exciting each port one at a time and monitoring the transmitted signal and signal received at each port, a complete 4×4 scattering matrix can be calculated, which fully characterizes

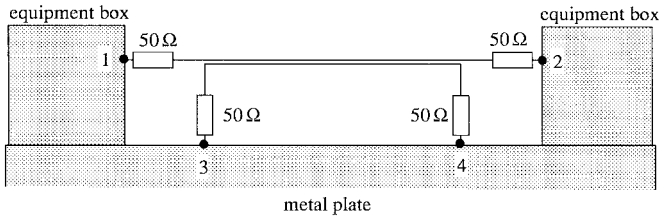

Fig. 7. Equipment box four-port structure.

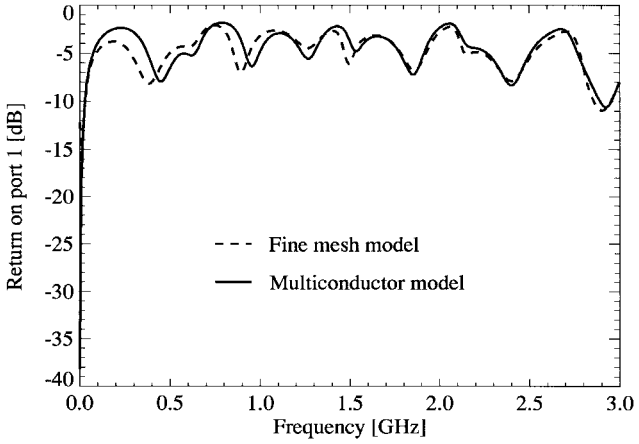

(a)

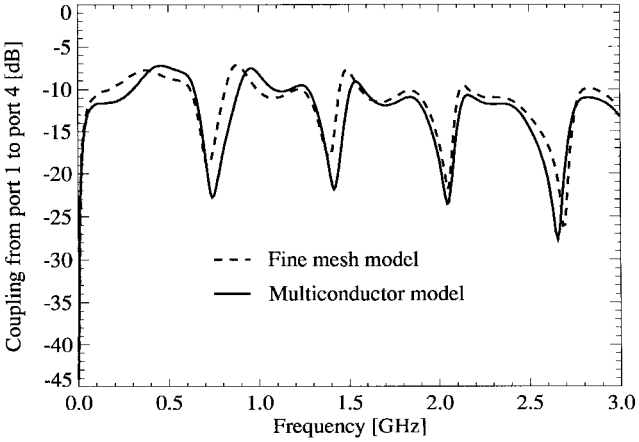

(b)

Fig. 8. (a) Return at equipment box port 1. (b) Coupling from port 1 at equipment box to port 4 on metal plate.

the electromagnetic coupling between the two wires on the metal structure.

Two sets of simulations have been performed, the first using the new multiconductor model and the second using a very fine TLM mesh in which the wires and loads are formed from solid cylindrical blocks of metal. Results are compared in Fig. 8(a) and (b). An excellent agreement between the two models, over a wide frequency range can be observed. It should be noted that the multiconductor model has required almost 60 times less central processing unit (CPU) time and memory than the fine mesh model.

As a further test of the multiconductor model, the magnetic field around a solenoid was simulated. The solenoid was 12-mm long with 6-mm diameter and consisted of 24 turns

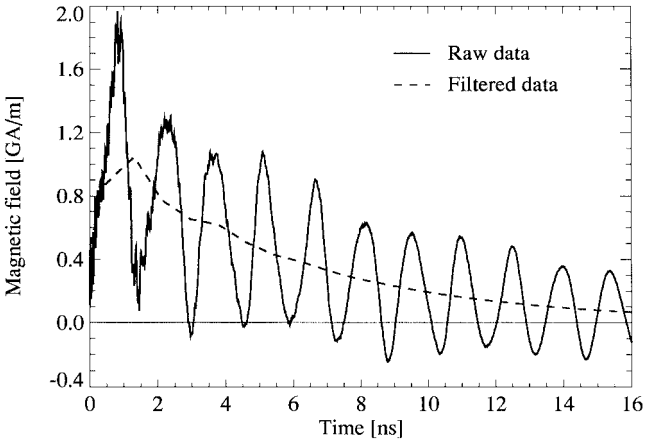

Fig. 9. Time response of magnetic field at the solenoid center.

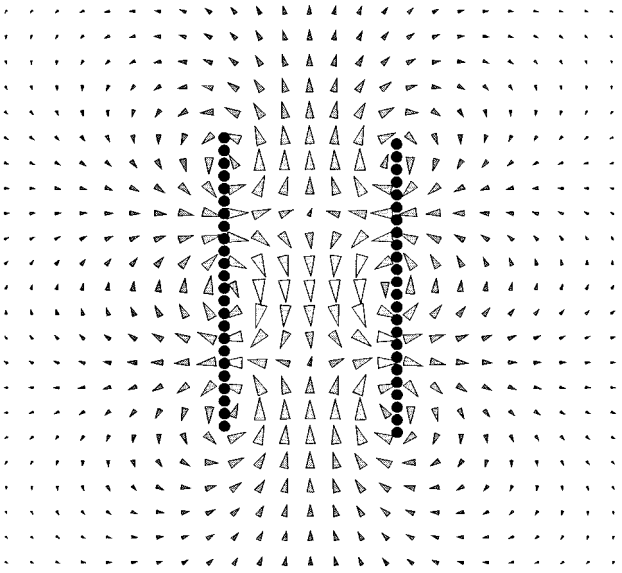

Fig. 10. Distribution of magnetic field at the first resonant frequency on a longitudinal section through the solenoid.

of 0.125-mm-diameter wire connected across a 330-Ω 1-V source. A regular 1-mm TLM mesh was used, so that on average the wire passed twice through each cell on its path. Note that as the wire passes from one layer of TLM cells to the next layer of cells along the solenoid axis, it effectively branches off of one loop of multiconductor and onto another. Thus, heavy use is made of both multiconductor bends and branches.

The computed time-domain magnetic field at the center of the solenoid is plotted in Fig. 9 (solid line). It exhibits a very low-frequency resonance and an exponentially decaying dc component. The resonance corresponds to one wavelength in the total length of wire in the circuit. This is confirmed in Fig. 10, which shows the magnetic field at resonance on a longitudinal section through the solenoid. Applying low-pass filtering, the resonant component of the field can be eliminated (Fig. 9, broken line), and the time constant of the dc component can be estimated. At around 5.54 ns, this corresponds to an inductance for the solenoid of about 1.83 μH—reasonably close to the analytic approximate for the solenoid (neglecting end-effects) of 1.71 μH.

V. Conclusion

Vector link lines and vector stub lines have been introduced in the TLM method to assist the development of a multiconductor model, integrated directly into the TLM time-stepping procedure. The new multiconductor TLM method allows for a self-consistent, efficient, and accurate modeling of coupling between the electromagnetic field and the multiconductor systems. The method is very general and can model multiconductor junctions, bends, and other complicated multiconductor configurations, as has been successfully demonstrated. In comparison to the fine mesh models, savings in computer resources are between one and two orders of magnitude.

References

[1] C. Christopoulos and P. Naylor, "Coupling between electromagnetic field and multiconductor transmission systems using TLM," *Int. J. Numer. Modeling*, vol. 1, pp. 7–17, 1988.
[2] A. Wlodarczyk and D. P. Johns, "New wire interface for graded 3-D TLM," *Electron. Lett.*, vol. 28, no. 8, pp. 728–729, Apr. 1992.
[3] J. A. Porti, J. A. Morente, M. Khalladi, and A. Gallego, "Comparison of thin-wire models for TLM method," *Electron. Lett.*, vol. 28, no. 20, pp. 1910–1911, Sept. 1992.
[4] C. R. Paul, *Analysis of Multiconductors Transmission Lines.* New York: Wiley, 1994.
[5] V. Trenkic and C. Christopoulos, "An efficient implementation of wire nodes in TLM," in *Proc. 2nd Int. Workshop on Transmission Line Matrix (TLM) Modeling*, Munich, Germany, 1997, pp. 60–67.

A. James Wlodarczyk was born in Bristol, U.K. He received the B.Sc. degree in electrical engineering and the Ph.D. degree from the University of Nottingham, Nottingham, U.K., in 1982 and 1988, respectively.

In 1988, he joined KCC Ltd., Nottingham, U.K., where he is currently a Research and Development Engineer.

Vladica Trenkic (S'92–M'95) was born in Aleksinac, Yugoslavia, in 1968. He received the Dipl.-Ing. degree in electrical engineering from the University of Niš, Niš, Yugoslavia, in 1992, and the Ph.D. degree from the University of Nottingham, Nottingham, U.K., in 1995.

In 1992, he joined the Department of Electrical and Electronic Engineering University of Nottingham, and spent five years working as a Research Associate. Since 1997, he has been with KCC Ltd. Nottingham, U.K., as a Research and Development Engineer. His research interests include numerical modeling using the transmission-line modeling method and its implementation to electromagnetic compatibility and microwave circuits.

Dr. Trenkic received the Institution of Electrical Engineers (IEE), U.K., Electronics Letters Premium Award in 1995.

Richard A. Scaramuzza was born in Huddersfield, U.K., in 1966. He received the B.Sc. degree in theoretical mechanics and the Ph.D. degree in electrical engineering from the University of Nottingham, U.K., in 1987 and 1993, respectively.

In 1992, he joined KCC Ltd. Nottingham, U.K., where he works in the development and implementation of TLM.

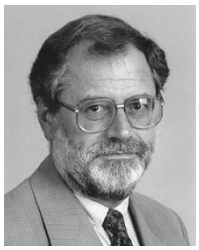

Christos Christopoulos (M'92) was born in Patras, Greece, in 1946. He received the Diploma in electrical and mechanical engineering from the National Technical University of Athens, Athens, Greece, in 1969, and the M.Sc. and D.Phil. degrees from the University of Sussex, Sussex, U.K., in 1970 and 1975, respectively.

In 1974, he joined the Arc Research Project, University of Liverpool, U.K., and spent two years working on vacuum arcs and breakdown while at UKAEA Culham Laboratories, U.K. In 1976, he joined the University of Durham, U.K., as a Senior Demonstrator in electrical engineering science. In October 1978, he joined the Department of Electrical and Electronic Engineering, University of Nottingham, Nottingham, U.K., where he is currently a Professor of electrical engineering. His research interests are in electrical discharges and plasmas, electromagnetic compatibility, electromagnetics, and protection and simulation of power networks.

Dr. Christopoulos received the Institution of Electrical Engineers (IEE), U.K., Snell Premium and IEE Electronics Letters Premium Awards in 1995.